Acta Pharmacologica Sinica

www.nature.com/aps

ARTICLE

JMJD6 protects against isoproterenol-induced cardiac hypertrophy via inhibition of NF-κB activation by demethylating R149 of the p65 subunit

Zhen Guo[1,2,3], Yue-huai Hu[2], Guo-shuai Feng[2,3], Carla Valenzuela Ripoll[3], Zhen-zhen Li[2], Si-dong Cai[2], Qian-qian Wang[2], Wen-wei Luo[2], Qian Li[2], Li-ying Liang[2], Zhong-kai Wu[4], Ji-guo Zhang[1], Ali Javaheri[3], Lei Wang[1]✉, Jing Lu[2]✉ and Pei-qing Liu[1,2]✉

Histone modification plays an important role in pathological cardiac hypertrophy and heart failure. In this study we investigated the role of a histone arginine demethylase, Jumonji C domain-containing protein 6 (JMJD6) in pathological cardiac hypertrophy. Cardiac hypertrophy was induced in rats by subcutaneous injection of isoproterenol (ISO, 1.2 mg·kg^{-1}·d^{-1}) for a week. At the end of the experiment, the rats underwent echocardiography, followed by euthanasia and heart collection. We found that JMJD6 levels were compensatorily increased in ISO-induced hypertrophic cardiac tissues, but reduced in patients with heart failure with reduced ejection fraction (HFrEF). Furthermore, we demonstrated that JMJD6 overexpression significantly attenuated ISO-induced hypertrophy in neonatal rat cardiomyocytes (NRCMs) evidenced by the decreased cardiomyocyte surface area and hypertrophic genes expression. Cardiac-specific JMJD6 overexpression in rats protected the hearts against ISO-induced cardiac hypertrophy and fibrosis, and rescued cardiac function. Conversely, depletion of JMJD6 by single-guide RNA (sgRNA) exacerbated ISO-induced hypertrophic responses in NRCMs. We revealed that JMJD6 interacted with NF-κB p65 in cytoplasm and reduced nuclear levels of p65 under hypertrophic stimulation in vivo and in vitro. Mechanistically, JMJD6 bound to p65 and demethylated p65 at the R149 residue to inhibit the nuclear translocation of p65, thus inactivating NF-κB signaling and protecting against pathological cardiac hypertrophy. In addition, we found that JMJD6 demethylated histone H3R8, which might be a new histone substrate of JMJD6. These results suggest that JMJD6 may be a potential target for therapeutic interventions in cardiac hypertrophy and heart failure.

Keywords: heart failure; cardiac hypertrophy; JMJD6; NF-κB; arginine demethylation; isoproterenol

Acta Pharmacologica Sinica (2023) 0:1–13; https://doi.org/10.1038/s41401-023-01086-7

INTRODUCTION

Cardiovascular disease (CVD) is a major public health challenge and the leading cause of mortality all around the world [1]. Pathological cardiac hypertrophy, which refers to the enlargement and thickening of the myocardial wall under various stress, injury, or stimulation, is an important independent risk factor for CVD [2, 3]. Although initially it can be a beneficial adaptive response that helps maintain normal cardiac function, sustained hypertrophy will eventually progress to heart failure [4]. Post-translational modifications serve as an important component of epigenetic modifications, which are widely involved in the development and progression of cardiac hypertrophy, and provide potential target for interventions aimed at reversing cardiac hypertrophy [5–9].

Recent developments in post-translational histone modifications, including newly discovered histone methylation modifications, have gained increasing attention in the treatment of various diseases [10]. Histone methylation mainly occurs on lysine and arginine residues, which can provide specialized binding surfaces that recruit protein complexes containing chromatin remodeling and transcriptional activation/repression activity, ultimately regulating gene expression [11, 12]. To date, multiple histone methyltransferases (HMTs) and demethylases (HDMs) have been identified [12], and their roles in diseases such as cancer [13], neurological disorders [14] and CVD [7, 15–17] (including cardiac hypertrophy and heart failure) have also been gradually revealed. Jumonji domain containing protein 2 A (JMJD2A) demethylates histone H3 lysine 9 trimethylation (H3K9me3) and activates transcription of pro-hypertrophic genes in mice [18]. We previously reported that JMJD3 promotes cardiac hypertrophy via decreasing H3K27me3 level in the promoter region of β-myosin heavy chain [19]. Recently, we found that protein arginine methyltransferase 5 (PRMT5) methylates histone H4 arginine 3 (H4R3) via symmetric di-methylation and protects against cardiac hypertrophy via regulation of Filip1L/β-catenin [15].

[1]School of Pharmaceutical Sciences, Shandong First Medical University & Shandong Academy of Medical Sciences, Taian 271016, China; [2]Department of Pharmacology and Toxicology, School of Pharmaceutical Sciences; National and Local United Engineering Lab of Druggability and New Drugs Evaluation; Guangdong Engineering Laboratory of Druggability and New Drug Evaluation; Guangdong Provincial Key Laboratory of New Drug Design and Evaluation, Sun Yat-sen University, Guangzhou 510006, China; [3]Center for Cardiovascular Research, Cardiovascular Division, Department of Medicine, Washington University School of Medicine, St. Louis, MO 63110, USA and [4]Department of Cardiac Surgery, First Affiliated Hospital, Sun Yat-sen University, Guangzhou 510080, China
Correspondence: Lei Wang (wanglei1118@sdfmu.edu.cn) or Jing Lu (lujing28@mail.sysu.edu.cn) or Pei-qing Liu (liupq@mail.sysu.edu.cn)
These authors contributed equally: Zhen Guo, Yue-huai Hu and Guo-shuai Feng

Received: 2 May 2022 Accepted: 2 April 2023
Published online: 25 April 2023

JMJD6, a member of the Jumonji C domain-containing family of proteins [20], contributes to the regulation of histone demethylation, transcriptional polymerase II promoter pause release and mRNA splicing through its ability to catalyze two types of reactions, lysyl hydroxylation and N-methyl argininyl demethylation [20–23]. Although the latter catalytic mechanism is controversial, it is of particular importance given that JMJD6 has been posited to be the only enzyme capable of catalyzing arginine demethylation. Moreover, there is compelling evidence that JMJD6 demethylates H3R2me2 and H4R3me2 and can affect gene expression in a locus-specific manner [20, 21]. Due to the complexity of its function, JMJD6 may also modify other histone substrates. In addition, JMJD6 can also demethylate non-histone proteins, such as ERα, G3BP1 and TRAF6 [24–26]. Our results show that JMJD6 is strongly related to cardiac hypertrophy and heart failure. Thus, it is necessary to fully understand the role of JMJD6 in this process, whether it is through the modification of histone arginine demethylation or through the modification of non-histone demethylation.

Nuclear factor kappa-B (NF-κB) is a redox-sensitive transcription factor family that regulates a series of inflammatory genes and plays an important role in the development of numerous pathological states [27]. Five members of the NF-κB family have been found in mammals: RelA (p65), p105/p50, p100/p52, RelB and c-Rel [28, 29]. The most common form in human cells is the p65/p50 heterodimer [28, 29]. In the canonical pathway of NF-κB activation, extracellular signals activate IκB kinase (IKK), which phosphorylates IκBα, leading to its ubiquitination and degradation by proteasomes. NF-κB, liberated from IκBα, translocates to the nucleus to regulate its target genes [28, 29]. An important aspect of NF-κB signaling regulation is multiple post-translational modifications of the p65 subunit [30]. Evidence indicates that lysine and arginine residues within NF-κB can be reversibly methylated by HMTs and HDMs [31]. To date, six methylated lysine sites (K37, K218, K221, K310, K314, and K315) [32–35] and one methylated arginine site (R30) [36] have been identified on the p65 subunit of NF-κB. Without exception, these methylation modifications regulate NF-κB activity and its target gene expression.

In the present study, we found that the mRNA and protein expression of JMJD6 were increased in isoproterenol (ISO)-induced cardiac hypertrophy in vivo and in vitro models, playing a protective role in pathological cardiac hypertrophy. Importantly, we showed that JMJD6 binds and demethylates NF-κB (p65) at R149 in the cytoplasm, which prevents the translocation of p65 into the nucleus, thereby reducing the activation of the NF-κB signaling pathway. Therapeutic approaches targeting JMJD6 may prove highly effective in preventing and treating pathological cardiac hypertrophy and heart failure via inhibition of NF-κB activity.

MATERIALS AND METHODS

Patient samples

This study includes heart samples from eight patients with heart failure that underwent heart transplantation. Three non-failing control heart tissues were obtained from prospective multi-organ donors, which did not exhibit cardiovascular pathology but were unable to be transplanted due to technical reasons. All patients or the family of prospective heart donors gave written informed consent prior to participation. The study was approved by the Human Ethics Committee of the First Affiliated Hospital of Sun Yat-sen University and followed the principles that govern the use of human tissues outlined in the Declaration of Helsinki.

Animal experiments

Sprague Dawley (SD) rats (male, weighing 220–240 g, SPF grade, Certification No. 44005800006028) were obtained from the Experimental Animal Center of Guangzhou University of Chinese Medicine (Guangzhou, China). SD rats were kept under controlled SPF environmental conditions (12:12 h light/dark cycle and room temperature 21–23 °C), with free access to water and standard chow. Recombinant adenovirus vectors encoding human JMJD6 cDNA (Ad-JMJD6, #VH843725) and Ad-Ctrl (pAd vector, serving as negative control) were purchased from Vigene Biosciences (Shandong, China). The direct gene delivery of JMJD6 or negative control was performed as previously described [37–40]. Briefly, SD rats were randomized into two groups, anesthetized by intraperitoneal (IP) injection with sodium pentobarbital (30 mg/kg), followed by endotracheal intubation and heart exposure. Then, 200 μL of Ad-JMJD6 or Ad-Ctrl (1×10^{10} particles) was injected into 4–6 sites around the left ventricular walls using sterile disposable insulin syringes (25-gauge needle, Bayon, Germany). Following injections, the thoracic incision was closed, and rats were administered gentamicin to prevent infection and meloxicam for analgesia. One week after adenovirus infection, rats were randomly assigned to receive either isoproterenol (ISO, purity > 98%, Tokyo Chemical Industry, Tokyo, Japan) or sterile normal saline (NS). Cardiac hypertrophy model was induced by subcutaneous (SQ) injection of ISO ($1.2\ mg \cdot kg^{-1} \cdot d^{-1}$) or NS in the vehicle control group, for 1 week according to our previous reports [19]. All animals and experimental procedures were approved by the Research Ethics Committee of Sun Yat-sen University and were performed following the Guide for the Care and Use of Laboratory Animals (NIH Publication No. 85–23, revised 1996). All the procedures were implemented in accordance with the China Animal Welfare Legislation, reviewed and approved by the Sun Yat-sen University Committee on Ethics in the Care and Use of Laboratory.

Cell culture, transfection and drug treatment

Primary culture of neonatal rat cardiomyocytes (NRCMs) were isolated from the hearts of 1–3 days old SD rats (Sun Yat-sen University) and cultured as previously described [19, 37, 40]. NRCMs were grown in Dulbecco's Modified Eagle's Medium (DMEM) supplemented with 10% (*v/v*) new born calf serum (NBCS), penicillin (100 U/mL)/streptomycin (100 μg/mL) (Thermo Fisher, #15140148, Waltham, MA, USA) and 100 μM 5-bromodeoxyuridine (Brdu) for 48 h, and then infected with lentivirus or recombinant adenoviruses. To induce hypertrophy, NRCMs were cultured in serum-free DMEM for 16 h and treated with ISO (10 μM) for 12 h. The control group cells were treated with the same volume of phosphate-buffered saline (PBS).

HEK293T cells were maintained in DMEM supplemented with 10% (*v/v*) FBS and penicillin/streptomycin and seeded into plates as needed for experiments. Plasmid transfections were performed using Lipofectamine LTX & Plus (Invitrogen, 15338100, Carlsbad, CA, USA) according to the manufacturer's instructions [19, 41].

Echocardiography analysis

Echocardiography was performed by a Technos MPX ultrasound system (ESAOTE, SpAESAOTE SpA, Italy) at the end of the trial according to our previous report [19, 37, 40–42]. Rats were anesthetized with 4% (*v/v*) isoflurane in the anesthetic chamber and then transferred to a heating pad for echocardiography with 2% isoflurane maintenance. After M-mode recording, basic cardiac function parameters were measured as followed: ejection fraction (EF), fractional shortening (FS), left ventricular end-systolic/diastolic internal diameter (LVID-s/d), left ventricular end-systolic/diastolic posterior wall thickness (LVPW-s/d) and end-systolic/diastolic interventricular septum (IVS-s/d) were measured. At the end of experiment, all the rats were euthanized by CO_2 inhalation, followed by heart collection.

Immunofluorescence (IF) assay

NRCMs were seeded and cultured on glass coverslips. After treatment, cells were fixed with 4% (*w/v*) paraformaldehyde for

10 min and permeabilized with 0.3% (*v*/*v*) TritonX-100 for 5 min at room temperature. After washing three times with PBS, the cells were blocked with 10% (*v*/*v*) goat serum at room temperature for 1 h, followed by incubation with individual primary antibodies overnight at 4 °C. The next day, the cells were washed and stained with Alexa Fluor-labeled secondary antibodies and DAPI. Immunofluorescence was analyzed with a confocal microscope (Carl Zeiss, LSM 710, Jena, Germany).

Histological analysis

For histological analysis, hearts were arrested with a 10% (*w*/*v*) potassium chloride (KCl) solution at end-diastole and then fixed in 4% (*w*/*v*) paraformaldehyde. Fixed hearts were embedded in paraffin and cut transversely into 5 μm sections. Serial heart sections were stained with Hematoxylin-eosin (H&E) or wheat germ agglutinin (WGA) to measure myocyte cross-sectional areas. The degree of collagen deposition was detected by picrosirius red (PSR) staining. Expression of JMJD6 was detected by immunohistochemistry (IHC) staining using the JMJD6 primary antibody, HRP-conjugated secondary antibody and DAB substrate.

For immunofluorescence, paraffin sections of cardiac samples were treated with individual primary antibodies overnight at 4 °C and followed by a standard IF assay.

Design of sgRNA and production of lentivirus

The sgRNA sequences of rat JMJD6 were designed using the Zhang laboratory website (https://zlab.bio/guide-design-resources) and the details of sequences were listed in Supplementary Table S1. Complementary oligonucleotides encoding sgRNA were annealed and cloned into *BsmB* I (NEB, Ipswich, MA, USA) sites in lentiC-RISPRv2 vectors (Addgene, Cambridge, MA, USA). HEK293T cells were co-transfected with lentiCRIS-PRv2-sgRNA construction, pMD2.G and psPAX2 by Lipofectamine LTX & Plus. Viral supernatants were harvested 48 h later and then filtered. The lentivirus of sgJMJD6 (JMJD6 knockdown) or Lenti-crispr v2 was aliquoted and stored at −80 °C.

Measurement of cell surface area

NRCMs cultured in 48-well plates were fixed with 4% (*w*/*v*) paraformaldehyde for 15 min, followed by 0.3% (*v*/*v*) TritonX-100 for 5 min at room temperature. Then the NRCMs were incubated with 0.1% (*w*/*v*) rhodamine-phalloidin (Invitrogen, #R415) for 30 min. After washing three times with PBS, the cells were stained with 4′, 6-diamidino-2-ph-enylindole (DAPI) (Invitrogen, #D1306) and inspected with a High Content Screening system (Thermo Fisher). The cell surface area was obtained from randomly selected fields and determined by the built-in image analysis software.

Real-time quantitative PCR (qRT-PCR)

Total RNA was extracted from NRCMs or cardiac tissues using TRIzol reagent (Invitrogen, #15596026). The first-strand cDNA was synthesized using First Strand cDNA Synthesis kit (Thermo Fisher, #11904018) and Quantitative PCR was performed with SYBR Green Master Mix (TOYOBO, #0810) using a Real-time Thermo Cycler (Thermo Fisher) to examine relative mRNA levels of indicated genes as previously described [19, 37]. Specific primers were synthesized by Sangon Biotech Co Ltd (Shanghai, China) and all PCR assays were done at least in triplicate. β-Actin (*ACTB*) was used as an endogenous control. Details of the sequences are listed in Supplementary Table S2.

Western blot analysis

Western blot was performed as previously described [19, 43, 44]. In brief, total protein was extracted from cells or tissues with RIPA lysis buffer (Beyotime Biotechnology, #P0013B, Shanghai, China) supplemented with protease inhibitor cocktail (Roche, #04693159001, Basel, Switzerland) and phosphatase inhibitor (Roche, #PHOSS-RO). Cardiac tissues were fractionated into nucleus-enriched and cytoplasmic samples by using a CelLytic NuCLEAR Extraction kit (Sigma, Nxtract), as previously described [45, 46]. Protein (15–50 μg) was separated by 8%–12% (*w*/*v*) sodium dodecyl sulfate polyacrylamide gel electrophoresis (SDS-PAGE) and transferred onto polyvinylidene fluoride (PVDF) membranes (Merck Millipore, #88518, Temecula, CA, USA). The membranes were blocked with 5% (*w*/*v*) non-fat milk and incubated overnight with individual primary antibodies. Then the membranes were washed and further treated with HRP-conjugated secondary antibodies at room temperature for 1 h. The immune complexes were visualized by enhanced chemiluminescence methods. The band intensity was measured and analyzed with NIH ImageJ software (Bethesda, MD, USA). The details of used primary and secondary antibodies were shown in Supplementary Table S3.

Co-immuoprecipitation (Co-IP) assay

Experiments were performed as previously described [41, 44, 47, 48]. Total protein (500 μg) was incubated with anti-JMJD6 (rabbit, diluted 1:50, Proteintech, #16476–1-AP, Rosemont, IL, USA) or anti-p65 (mouse, diluted 1:100, CST, 6956, Danvers, MA, USA) antibodies overnight (normal IgG was used as control), and incubated with protein A/G-agarose beads (Pierce, #20421, Rockford, IL, USA) at 4 °C for 4 h. Afterward, the beads were washed with lysis buffer for 3 times and immunoprecipitates were eluted by adding 35 μL of 1× sample buffer, boiled for 10 min at 95 °C, and centrifuged at 13000 rpm for 5 min. Then the supernatant was subjected to a standard Western blot assay.

Plasmid construction and mutation

To obtain a vector overexpressing rat JMJD6 (WT-JMJD6), NF-κB (p65) (WT-p65) or PRMT5 (WT-PRMT5), the rat *JMJD6* (GI: 1259883802), *NF-κB (p65)* (GI: 32187084) or *PRMT5* (GI: 184150975) expression vector was constructed by ligating corresponding full-length cDNA into a pcDNA3.1 expression vector (Generay Biotech, Shanghai, China). The mutation of JMJD6 at histidine 187 (JMJD6-H187A), aspartic acid 189 (JMJD6-D189A) or double mutant of site 187 and 189 (JMJD6-Double) and p65 at arginine 30 (p65-R30A), 149 (p65-R149A), 236 (p65-R236A) or 336 (p65-R336A) were generated by PCR using Fast Mutagenesis System (TransGen, #FM111-01, Beijing, China). Specific mutated primers were designed using the PrimerX website (https://www.bioinformatics.org/primerx/) as shown in Supplementary Table S4. All the plasmids were validated by DNA sequencing in Sangon Biotech Co. Ltd (Shanghai, China).

Methlyation site prediction of NF-κB (p65)

According to a published study, Wei at al showed that PRMT5 could dimethylate arginine (R) at the site R30 position of the p65 subunit [36]. We wanted to further explore if other arginine sites could be methylated. Thus, we used an online methylation site prediction platform (http://msp.biocuckoo.org/online.php) [49] to screen the potential arginine methylation sites in amino acid sequence of *Rattus norvegicus* NF-κB (p65) by setting the threshold.

Statistical analysis

All data are presented as the mean ± SEM and analyzed using Prism Version 9.0.0 (GraphPad Software Inc). Data were tested for assumptions of normality with the Shapiro-Wilk normality test. If the samples were normally distributed, a parametric statistical analysis was performed using unpaired 2-tailed Student's *t* test for 2 group comparisons or one-way analysis of variance (ANOVA) to determine mean differences between multiple groups; where appropriate, *post hoc* testing with Tukey test for multiple pairwise comparisons was used. If the samples were not normally distributed, we performed Kruskal-Wallis testing for multiple group analysis with Dunn post hoc testing or Mann-Whitney testing for 2 groups. In all analyses, a value of $P < 0.05$ was considered statistically significant.

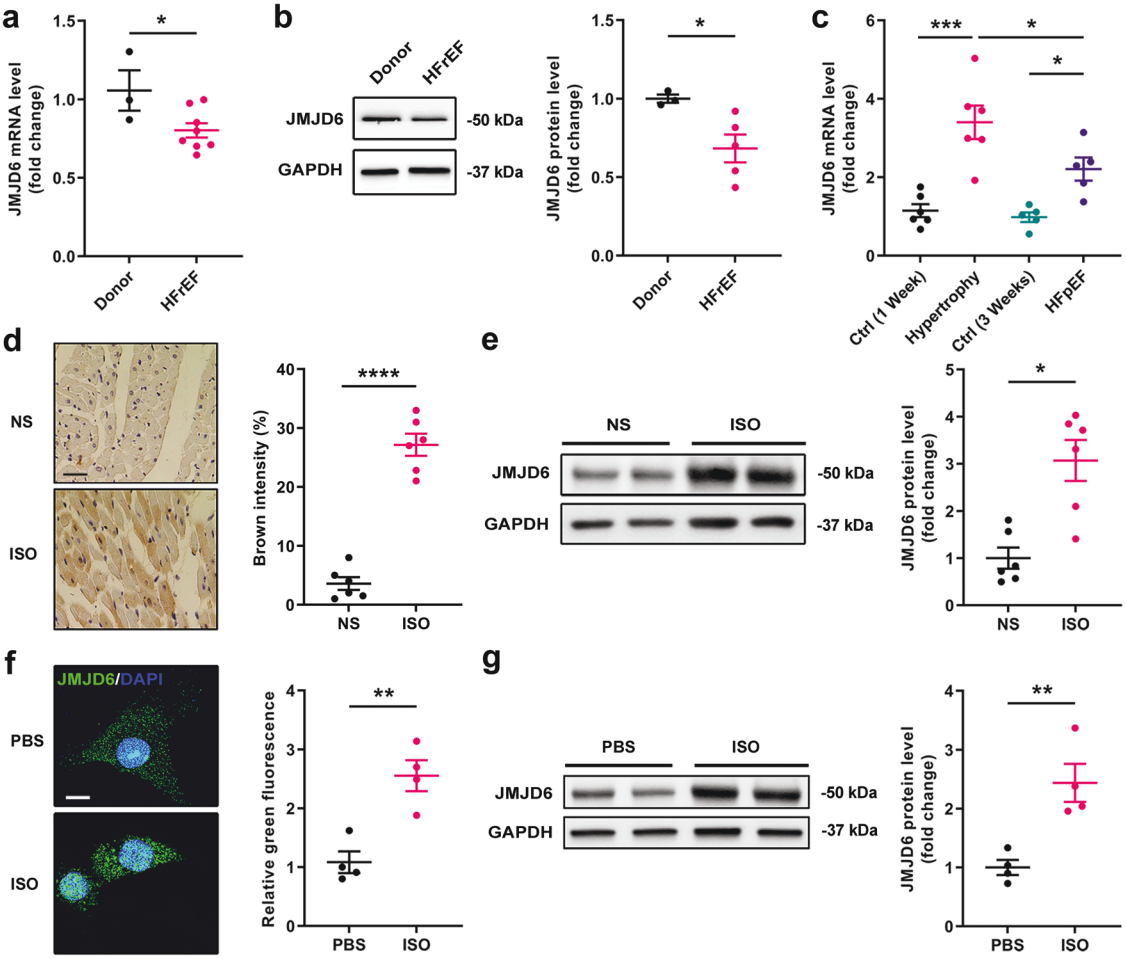

Fig. 1 JMJD6 expression was changed in HFrEF patients and hypertrophic rat hearts. a The mRNA level of JMJD6 in non-failing controls (Donor) or heart failure with reduced ejection fraction (HFrEF) patients ($n = 3$ in Donor group, $n = 8$ in HFrEF group). **b** The protein level of JMJD6 in Donor control or HFrEF patients ($n = 3$ in Donor group, $n = 5$ in HFrEF group). **c** The mRNA level of JMJD6 in ISO-induced hypertrophic cardiac tissues (1.2 mg·kg^{-1}·d^{-1} × 7 days, SQ, $n = 6$) and heart failure with preserved ejection fraction (HFpEF) cardiac tissues (2.5 mg·kg^{-1}·d^{-1} × 21 days, IP, $n = 5$). **d** The protein expression of JMJD6 in ISO-induced hypertrophic cardiac tissues was shown as brown intensity by immunohistochemistry staining, scale bar = 30 μm ($n = 6$). **e** The protein level of JMJD6 in ISO-induced hypertrophic cardiac tissues was shown by Western blot analysis ($n = 6$). **f** The protein expression of JMJD6 in ISO-induced NRCMs was identified by confocal immunofluorescence microscopy, scale bar = 10 μm ($n = 4$). **g** The protein expression of JMJD6 in ISO-induced NRCMs was identified by Western blot analysis ($n = 4$). Student's *t* test was used in (**a**), (**b**) and (**d**–**g**), One-way ANOVA with Tukey's correction for multiple comparisons was used in (**c**). $^{*}P < 0.05$, $^{**}P < 0.01$, $^{***}P < 0.001$, $^{****}P < 0.0001$. NS normal saline, PBS phosphate-buffered saline.

RESULTS

JMJD6 expression was changed in HFrEF patients and hypertrophic rat hearts

We have previously demonstrated a novel role of JMJD3 (a histone demethylase) in promoting cardiac hypertrophy via decreasing H3K27me3 level in the promoter region of β-myosin heavy chain [19]. To more comprehensively assess the transcriptional levels of the JMJD family in an ISO-induced cardiac hypertrophy murine model, as evidenced by echocardiography analysis and morphometric measurement (Supplementary Table S5, Supplementary Fig. S1a–d), we employed qRT-PCR to detect the mRNA expression of JMJD subtypes in cardiac tissues. These results show that the transcriptional levels of multiple JMJD subtypes were significantly altered, with JMJD6 being the most prominent subtype (Supplementary Fig. S1e).

To further determine whether JMJD6 is pathophysiologically relevant to the progression of heart failure, we firstly examined cardiac mRNA and protein levels of JMJD6 in patients with HF with reduced ejection fraction (HFrEF) undergoing heart transplantation. We observed that JMJD6 mRNA and protein levels were remarkably reduced in patients with HFrEF (mean EF ~22.2%, Supplementary Fig. S2) compared to non-failing donors (Fig. 1a, b). In murine model, we examined the mRNA level of JMJD6 in ISO-induced cardiac hypertrophic rats with increased EF (64.5–81.9%, Supplementary Table S5), as well as in ISO-induced HF with preserved ejection fraction (HFpEF) rats with decreased EF (65.7% to 51.8%, Supplementary Table S6). Compared with control rats, the mRNA level of JMJD6 was dramatically increased in cardiac hypertrophy (3.4-fold) and HFpEF (2.2-fold) rats (Fig. 1c). Meanwhile, JMJD6 protein level was also significantly increased in hypertrophic rat hearts, as shown by IHC staining (Fig. 1d) and Western blot analysis (Fig. 1e). Similarly, both mRNA and protein levels of JMJD6 were obviously elevated in ISO-treated NRCMs (Fig. 1f, g, Supplementary Fig. S3), which was consistent with in vivo results. Moreover, JMJD6 protein level was also increased in transverse aortic constriction (TAC) mice model (Supplementary Fig. S4).

JMJD6 negatively correlated with ISO-induced cardiac hypertrophy in NRCMs

We then wanted to investigate the role of JMJD6 in the regulation of ISO-induced cardiac hypertrophy by using the gain- and

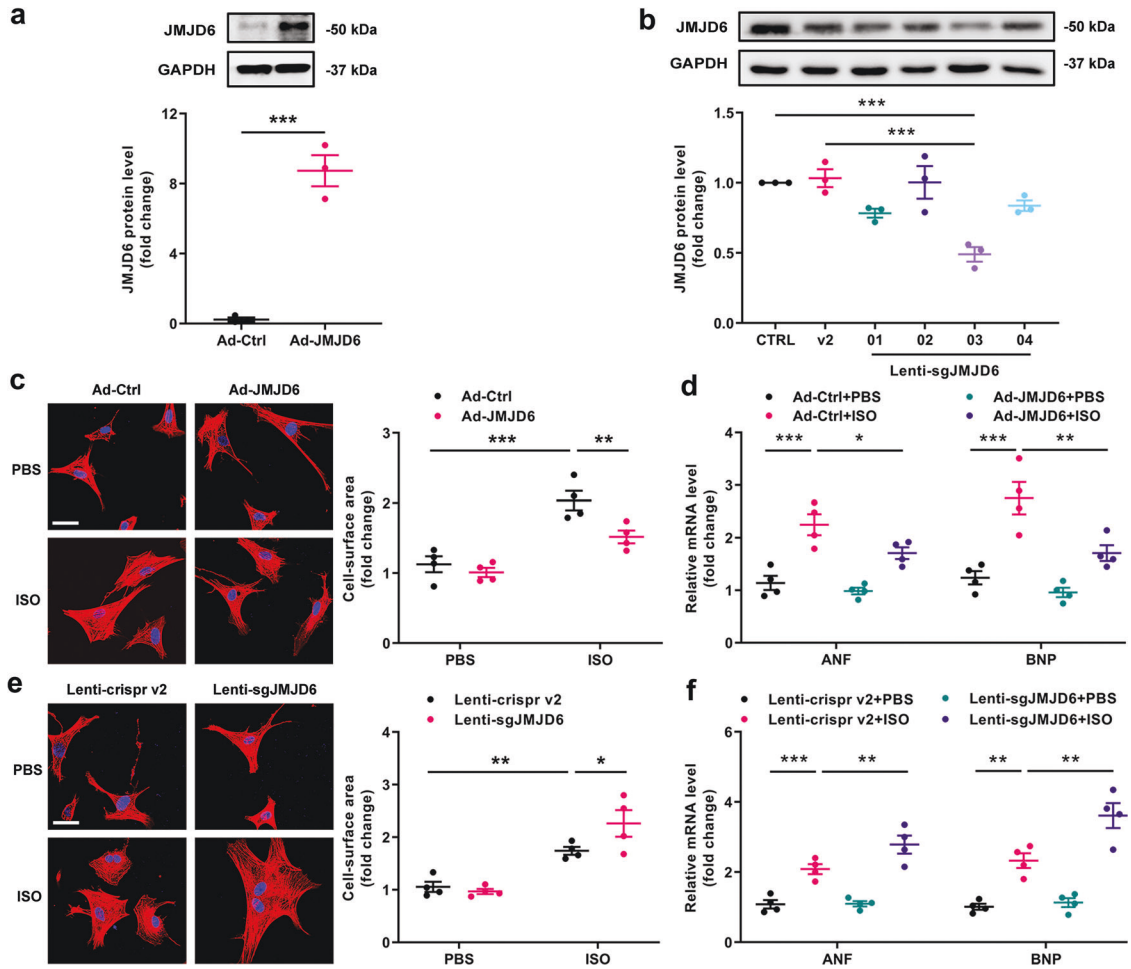

Fig. 2 JMJD6 negatively regulates ISO-induced cardiac hypertrophy in NRCMs. a The adenovirus infection efficiency was confirmed by Western blot in NRCMs infected with Ad-Ctrl (empty vector) or Ad-JMJD6 ($n = 3$). **b** JMJD6 protein level was detected by Western blot in NRCMs infected with Lenti-crispr v2 (empty vector) or Lenti-sgJMJD6-01, 02, 03 or 04 ($n = 3$). **c** Cell surface area was measured by rhodamine-phalloidin staining in NRCMs infected with Ad-Ctrl or Ad-JMJD6 for 48 h in the presence of ISO (10 μM, 12 h) or PBS, scale bar = 20 μm ($n = 4$). **d** The mRNA level of hypertrophic genes (ANF and BNP) in NRCMs infected with Ad-Ctrl or Ad-JMJD6 ($n = 4$). **e** Cell surface area was measured in NRCMs infected with Lenti-crispr v2 or Lenti-sgJMJD6, scale bar = 20 μm ($n = 4$). **f** The mRNA level of hypertrophic genes in NRCMs infected with Lenti-crispr v2 or Lenti-sgJMJD6 ($n = 4$). Student's *t* test was used in (**a**), One-way ANOVA with Tukey's correction for multiple comparisons was used in (**b**–**f**). $^{*}P < 0.05$, $^{**}P < 0.01$, $^{***}P < 0.001$. Ad-Ctrl control adenovirus, Ad-JMJD6 adenovirus overexpressing JMJD6, ANF atrial natriuretic factor, BNP brain natriuretic polypeptide. Lenti-sgJMJD6 means Lenti-sgJMJD6-03.

loss-of-function approaches in vitro. One group of NRCMs was infected with Ad-JMJD6 (overexpression) or Ad-Ctrl (control), while another group of NRCMs was infected with Lenti-sgJMJD6 (knockdown) or Lenti-crispr v2 (empty vector). The efficiency of Ad-JMJD6 (Fig. 2a) or Lenti-sgJMJD6 (Fig. 2b) in NRCMs was verified by Western blot analysis. JMJD6-03 has the best efficiency, hereafter referred to as Lenti-sgJMJD6. ISO treatment led to pronounced enlargement of cell surface area (Fig. 2c, e) and upregulation of hypertrophic markers, including ANF and BNP (Fig. 2d, f). These hypertrophic responses induced by ISO were significantly attenuated by JMJD6 overexpression with Ad-JMJD6 infection (Fig. 2c, d). In contrast, JMJD6 knockdown by Lenti-sgJMJD6 infection aggravated ISO-induced hypertrophic responses (Fig. 2e, f). However, Ad-JMJD6 or Lenti-sgJMJD6 infection did not affect the hypertrophic response under normal physiological conditions. These results suggest that JMJD6 protects against ISO-induced cardiac hypertrophy in vitro.

JMJD6 overexpression attenuated ISO-induced cardiac hypertrophy in rats

Given the protective role of JMJD6 on ISO-induced cardiac hypertrophy in vitro, we further investigated whether JMJD6 overexpression in cardiomyocytes could rescue cardiac function in vivo. To this end, Ad-JMJD6 was directly administered into the left ventricle of SD rats via intramyocardial injection to achieve cardiac-specific JMJD6 overexpression, while control rats received Ad-Ctrl. One week post-infection, rats were injected with ISO (1.2 $mg \cdot kg^{-1} \cdot d^{-1}$, IP) for 7 days. Results from the IHC staining and Western blot analysis in heart tissue confirmed that the overexpression of JMJD6 was successful (Supplementary Fig. S5). When rats that received Ad-Ctrl injection were subjected to ISO treatment, they developed cardiac hypertrophy, as evidenced by echocardiographic analysis (Fig. 3a, b, Supplementary Fig. S6), increased heart size (Fig. 3c), increased heart weight-to-body weight (HW/BW) and heart weight-to-tibia length (HW/TL) ratios (Fig. 3d). Staining results of Hematoxylin-Eosin (H&E), wheat germ agglutinin (WGA) and picrosirius red (PSR) demonstrated that ISO treatment increased cardiomyocyte size and fibrosis in Ad-Ctrl rats (Fig. 3e, f). Remarkably, these hypertrophic features were attenuated in the hearts of rats that received Ad-JMJD6 injection and treatment with ISO (Fig. 3a–e, Supplementary Fig. S6). Furthermore, Ad-JMJD6 injection also significantly ameliorated fibrosis in hypertrophic hearts, as seen in PSR staining (Fig. 3f). Consistently, qRT-PCR results showed that mRNA levels of

hypertrophic genes, including ANF and BNP, and fibrotic genes including COL1A1, COL3A1 and CTGF, were attenuated by JMJD6 overexpression in heart tissue exposed to ISO (Fig. 3g, h), suggesting that JMJD6 repressed ISO-induced cardiac hypertrophy and fibrosis in rats. These data, along with alterations of JMJD6 levels in different animal models and patients, suggest that JMJD6 may be a beneficial compensatory factor in the process of pathological cardiac hypertrophy.

JMJD6 regulated NF-κB (p65) signaling in ISO-induced cardiac hypertrophy

Nuclear factor κB (NF-κB) is often implicated in contributing to the detrimental effects of cardiac injury [50]. We and others have proved that the activity of NF-κB is increased under hypertrophic stimulation, including ISO treatment [41, 51–53]. In our current study, we observed physiological binding between JMJD6 and NF-κB p65 in NRCMs. More importantly, ISO treatment induced a marked increase of this interaction (Fig. 4a, b). Analysis of IF staining shows that nuclear p65 is increased in NRCMs exposed to ISO, but this rise is attenuated in cells that overexpress JMJD6. Interestingly, co-localization of JMJD6 and p65 protein in the cytoplasm was significantly increased in the Ad-Ctrl group treated with ISO, however, in the JMJD6 overexpression group there was significant elevation from baseline which further increased when exposed to ISO (Fig. 4c). These results indicate that overexpression of JMJD6 could inhibit the translocation of p65 into the nucleus. Moreover, analysis of cytonuclear fractions shows that JMJD6 overexpression reversed ISO-induced increases in the nucleus/cytoplasm p65 (Fig. 4d). These results suggest that NF-κB signaling is regulated by JMJD6 in cardiac hypertrophy.

Murine hearts also show interaction between nuclear and cytoplasmic p65 with JMJD6 in vivo (Fig. 5a), which is consistent with the results of NRCMs in vitro. In addition, the ratio of phosphorylated p65 at Ser536 to total p65 (p-p65/p65) is an important index of NF-κB signaling activation [54, 55], and we observed that the Ad-Ctrl infection group had a distinct increase of the p-p65/p65 ratio, indicating the activation of NF-κB signaling in ISO-induced cardiac hypertrophy (Fig. 5b). However, Ad-JMJD6 infection effectively attenuated ISO-induced elevations of p-p65/p65 ratio (Fig. 5b). Of note, Ad-JMJD6 infection did not significantly alter the expression of IκBα after ISO treatment (Fig. 5b), which indicates the degradation of IκBα was not affected. Furthermore, we found that overexpression of JMJD6 does not affect baseline expression of IκBα in vivo or in vitro (Fig. 5b, c). Taken together, these results demonstrate that JMJD6 participates in the protective effect of ISO-induced cardiac hypertrophy by inhibiting the translocation of p65 into the nucleus, rather than inhibiting the degradation of IκBα.

JMJD6 decreased the methylation level in ISO-induced cardiac hypertrophy

JMJD6 is the first demethylase that has been demonstrated to have demethylation enzyme activity on histone H3 at arginine 2 (H3R2) and H4R3 [20]. Despite there being multiple reports that show that JMJD6 acts as a demethylase to modify histone or non-histone arginine residues, there is still controversy surrounding JMJD6' demethylation ability [20, 21, 24–26]. Due to the dispute over the function of JMJD6, we first wanted to verify whether JMJD6 presents the demethylase activity in cardiomyocytes. To address this question, we used PRMT5 (a recognized protein arginine methyltransferase, which catalyzes monomethylation and symmetrical dimethylation of arginine on H4R3 and H3R8) to serve as a positive control. To test whether the enzymatic activity of JMJD6 was involved in this process, we used an enzyme mutated plasmid, where the proposed Fe (II)-binding residues in JMJD6 were substituted with non-chelating residues (JMJD6-H187A, D189A or H187A/D189A (Double)) to abolish both the histone demethylase and hydroxylase activity [20, 26]. We found that overexpression of PRMT5 increased the levels of H4R3me1, H4R3me2s, H3R8me1 and H3R8me2s (Fig. 6a, b), indicating that PRMT5 promoted the methylation of histone substrate of H4R3 and H3R8. We also found that transfection of WT-JMJD6 could reduce the levels of H4R3me1 and H3R8me1, but did not decrease the levels of H4R3me2s and H3R8me2s (Fig. 6a, b). More importantly, the mutant JMJD6 showed no reductions of H4R3 and H3R8 levels. Therefore, these results indicate that JMJD6 does have demethylation function and H3R8 may be its new histone substrate.

Next, we investigated the arginine methylation level after ISO treatment in NRCMs. Interestingly, we observed increased expression of monomethylation and symmetrical dimethylation of arginine (Supplementary Fig. S7), indicating that ISO stimulation elevated overall arginine methylation levels. This result seems to contradict the up-regulation of JMJD6 expression after ISO stimulation, where we would expect reduced methylation levels. However, overall methylation levels can be regulated by both demethylases and methyltransferases, which could explain this up-regulation. Instead, we were more concerned about the effect of JMJD6 overexpression on the overall methylation caused by ISO stimulation. Based on our current results, we confirmed that JMJD6 overexpression can indeed reduce methylation levels induced by ISO in NRCMs (Fig. 6c, d).

JMJD6 demethylated R149 of p65 to inactivate NF-κB in ISO-induced cardiac hypertrophy

To explore whether JMJD6 exerts a protective effect in cardiac hypertrophy by demethylating p65 (a new partner of JMJD6), we first verified the possibility of methylation modification of p65. Using Co-IP analysis with an antibody against p65, we found that p65 can undergo arginine monomethylation and symmertrical demethylation (Fig. 7a), which is consistent with a previous study that PRMT5 dimethylates p65 [36]. In their study, PRMT5 dimethylates R30 of the p65 subunit to activate NF-κB [36]. Considering our current findings, we further hypothesized whether JMJD6 also inactivates NF-κB to play a protective role by demethylating p65 at R30 or other sites. To this end, we screened the potential arginine methylation sites in amino acid sequences of *Rattus norvegicus* p65 using a methylation site prediction platform. According to the screening analysis, we found that no potential methylation sites appeared when the threshold was set to 0.9 (Fig. 7b). However, when the threshold continued to decrease, we obtained a series of potential methylation sites, such as R30, R149, R236 and R336 (Fig. 7b). Interestingly, these potential sites (except R336) existed conservatively among different species, and they also have similar amino acid sequence characteristics, that is, arginine (R) was always accompanied by a glycine (G) (Supplementary Table S7), indicating that this may be a special domain required for methylation modification. Therefore, we used R30 as a control to explore the function of other potential sites in our experiments. Co-transfection with WT-JMJD6 and p65 (WT or four different mutants) in 293 T cells showed that the ratio of p-p65/p65 was the same compared between WT-p65 and R30A-p65 in the presence of WT-JMJD6, but it was markedly increased in R149A-p65 transfection (Fig. 7c). This result indicates that demethylation at R149 of p65 inhibits the activity of p65, which may be due to the demethylation of JMJD6 at p65 (R149) leading to reductions of p65 translocation into the nucleus. In addition, we also observed the effect of WT-PRMT5 on p-p65 by co-transfection with WT-PRMT5 and p65 (WT or four different mutants). The results showed that the ratio of p-p65/p65 was significantly decreased in R30A-p65 in the presence of WT-PRMT5 (Fig. 7d), indicating that PRMT5 methylates R30 of p65 subunit to activate NF-κB. Thus, methylation/demethylation of p65 can exist at different sites in a context-dependent manner.

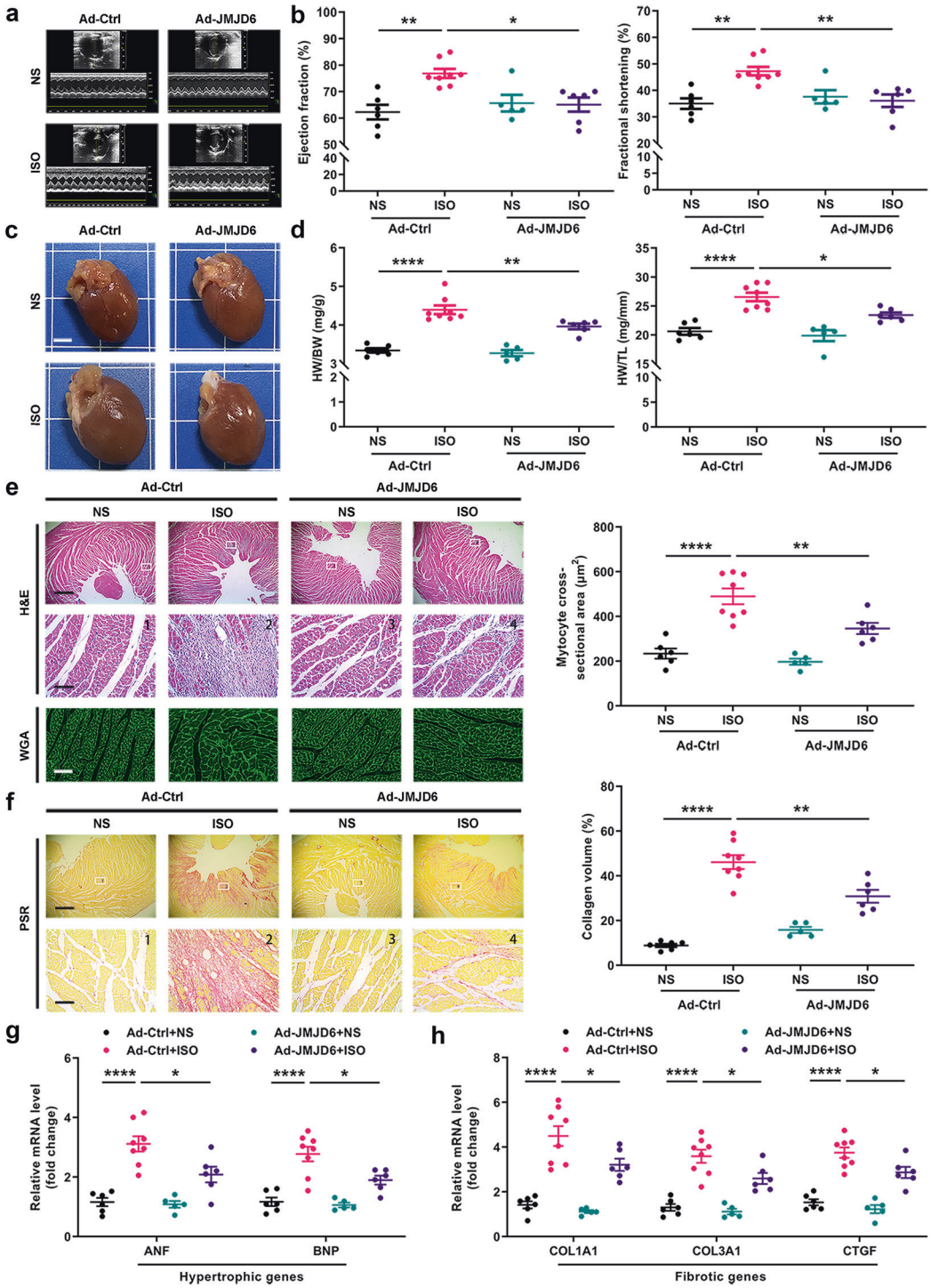

Fig. 3 JMJD6 overexpression represses ISO-induced cardiac hypertrophy in rats. a Representative echocardiography of SD rats infected with Ad-Ctrl or Ad-JMJD6 for 14 days in the presence of ISO or NS. **b** Ejection fraction (EF) and fractional shortening (FS) of Ad-Ctrl or Ad-JMJD6 infected rats treated with ISO or NS ($n = 5–8$). **c** Representative heart morphology of SD rats infected with Ad-Ctrl or Ad-JMJD6 for 14 days in the presence of ISO or NS, scale bar = 2 mm. **d** Heart weight-to-body weight (HW/BW) ratios and HW to-tibia length (HW/TL) ratios of Ad-Ctrl or Ad-JMJD6 infected rats treated with ISO or NS ($n = 5–8$). **e** Hematoxylin-Eosin (H&E, scale bar = 1 mm or 50 μm) and wheat germ agglutinin (WGA, scale bar = 50 μm) staining were performed to determine the cardiomyocyte size of Ad-Ctrl or Ad-JMJD6 infected rats treated with ISO or NS ($n = 5–8$). **f** Picrosirius red (PSR, scale bar = 1 mm or 50 μm) staining was performed to determine cardiac fibrosis of the hearts from Ad-Ctrl or Ad-JMJD6 infected rats treated with ISO or NS ($n = 5–8$). **g** The mRNA levels of hypertrophic genes in Ad-Ctrl or Ad-JMJD6 infected rats treated with ISO or NS ($n = 5–8$). **h** The mRNA levels of fibrotic genes (COL1A1, COL3A1 and CTGF) in Ad-Ctrl or Ad-JMJD6 infected rats treated with ISO or NS ($n = 5–8$). Kruskal-Wallis test with Dunn's post-hoc for multiple comparisons was used in panel (**b**) for ejection fraction, One-way ANOVA with Tukey's correction for multiple comparisons was used in (**b**) for fractional shortening and (**d**–**h**). $^{*}P < 0.05$, $^{**}P < 0.01$, $^{****}P < 0.0001$. COL1A1 collagen1a1, COL3A1 collagen3a1, CTGF connective tissue growth factor.

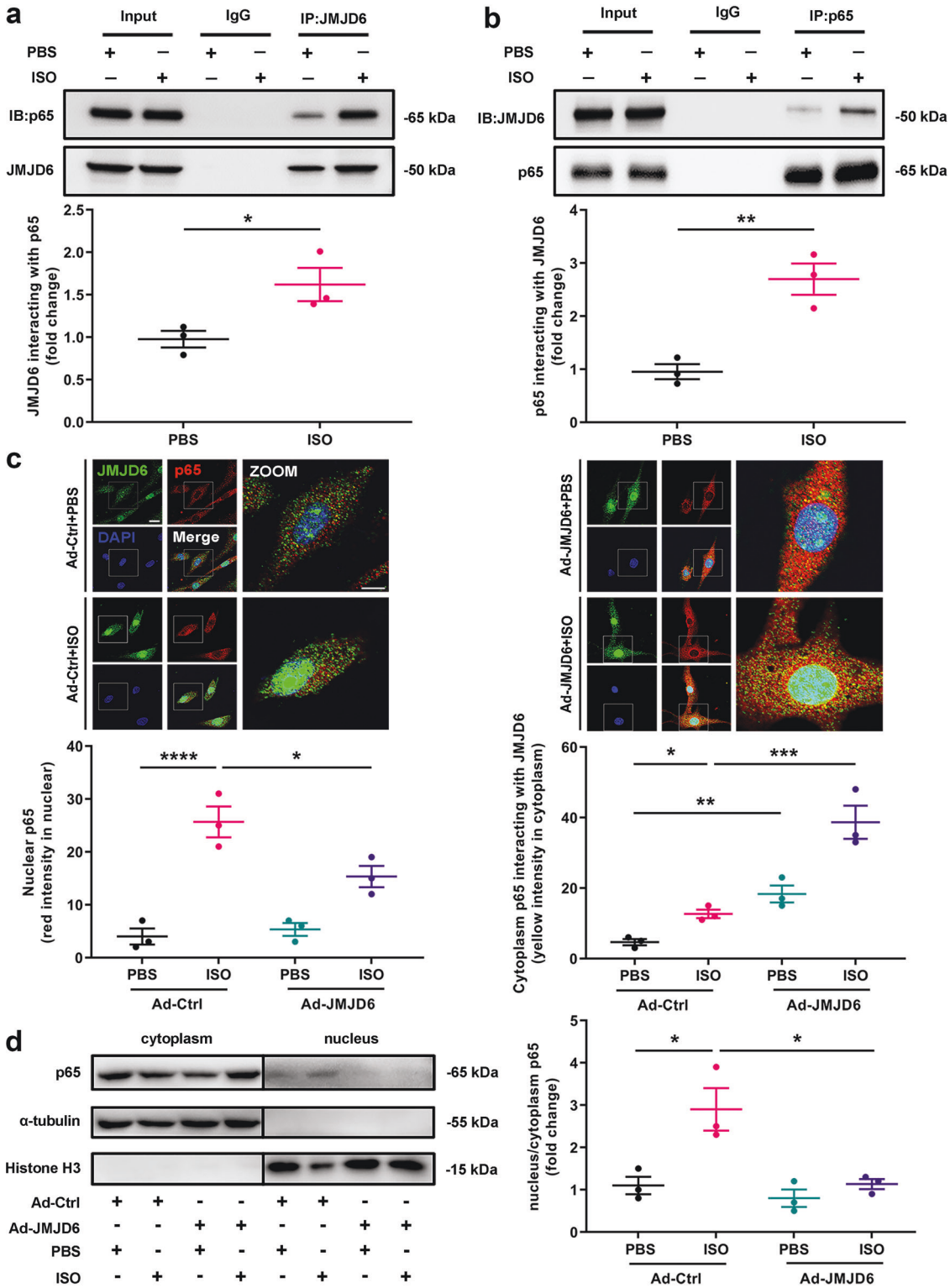

Fig. 4 JMJD6 regulates NF-κB signaling in ISO-induced cardiac hypertrophy in vitro. a Immunoprecipitation analysis showed that interaction of p65 and JMJD6 in NRCMs using JMJD6 antibody in presence of ISO or PBS ($n = 3$). **b** Immunoprecipitation analysis showed that interaction of JMJD6 and p65 in NRCMs using p65 antibody in presence of ISO or PBS ($n = 3$). **c** Subcellular location of p65 in NRCMs. NRCMs were infected with Ad-JMJD6 or Ad-Ctrl for 24 h in presence of ISO or PBS, followed by immunofluorescence to detect the JMJD6 and p65 protein. Upper: Representative immunofluorescence showing the location of JMJD6 (green) and p65 (red), scale bar = 25 μm or 10 μm. Lower: Blinded quantification of nuclear p65 and cytoplasmic p65 interacting with JMJD6 ($n = 3$). **d** The protein expression of p65 was measured by Western blot analysis in the cytoplasm and nucleus in NRCMs infected with Ad-Ctrl or Ad-JMJD6 for 24 h in the presence of ISO or PBS. Left: Representative Western blot images showing the level of p65. Right: The quantification of nucleus/cytoplasm p65 ($n = 3$). Student's *t* test was used in (**a**) and (**b**), One-way ANOVA with Tukey's correction for multiple comparisons was used in (**c**) and (**d**). $^{*}P < 0.05$, $^{**}P < 0.01$, $^{***}P < 0.001$, $^{****}P < 0.0001$.

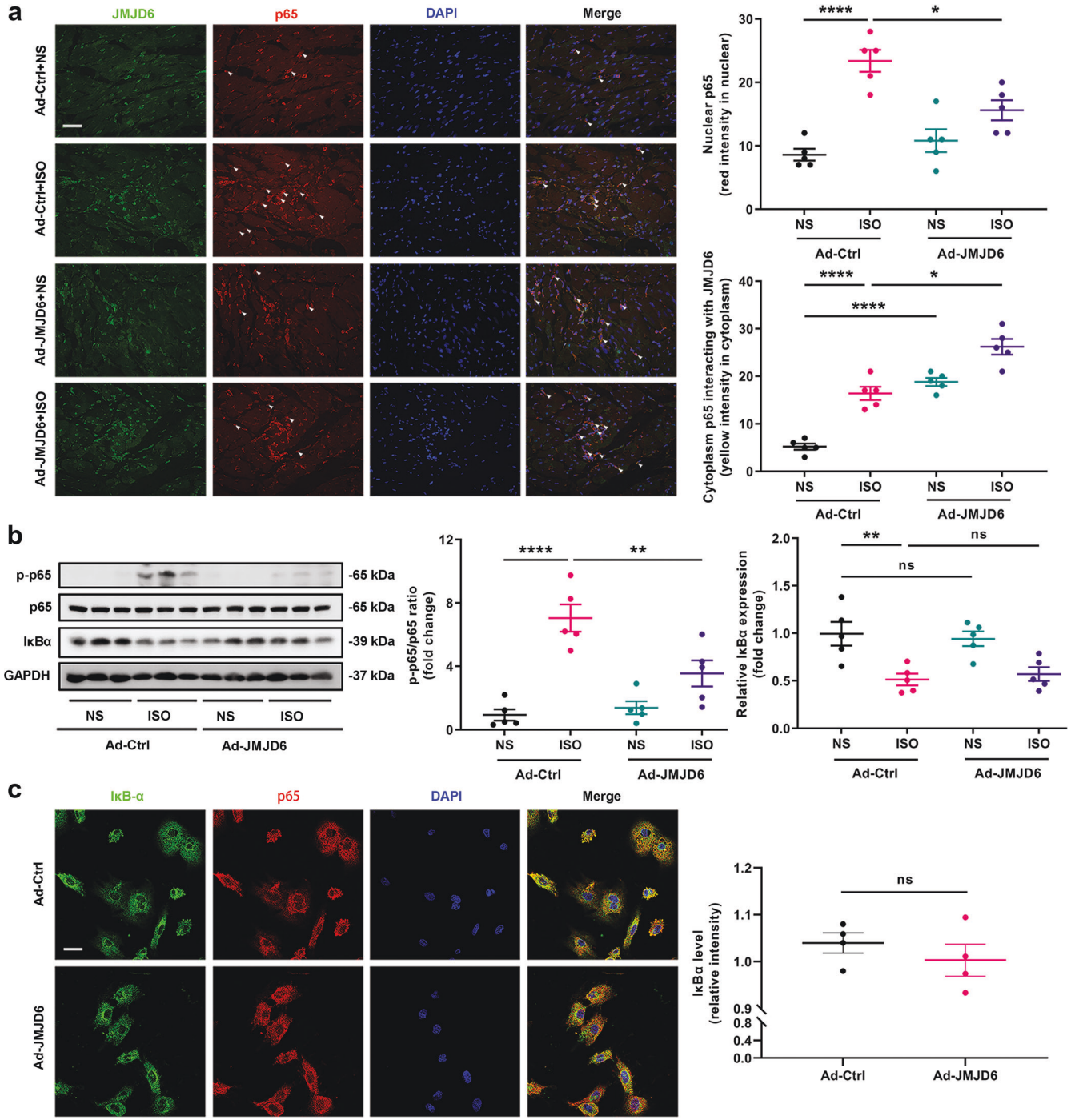

Fig. 5 JMJD6 regulates NF-κB signaling in ISO-induced cardiac hypertrophy in vivo. a Immunofluorescence analysis showed that the expression of p65 and JMJD6 in SD rats infected with Ad-Ctrl or Ad-JMJD6 for 14 days in the presence of ISO or NS. Left: Representative immunofluorescence showing the location of JMJD6 (green) and p65 (red), scale bar = 50 μm. Right: Blinded quantification of nuclear p65 and cytoplasmic p65 interacting with JMJD6 ($n = 5$). **b** Representative Western blot images and quantitative results showing p65 phosphorylation at Ser536 and relative IκBα expression in cardiac tissues of Ad-Ctrl or Ad-JMJD6 infection for 14 days in the presence of ISO or NS ($n = 5$). **c** Immunofluorescence analysis showed that the expression of IκBα (green) and p65 (red) in NRCMs infected with Ad-Ctrl or Ad-JMJD6 for 24 h, scale bar = 25 μm ($n = 4$). One-way ANOVA with Tukey's correction for multiple comparisons was used in (**a**) and (**b**), Student's *t* test was used in (**c**). $^{*}P < 0.05$, $^{**}P < 0.01$, $^{****}P < 0.0001$, ns not significant.

DISCUSSION

The most significant finding in the present study is that JMJD6 has a protective effect on cardiac hypertrophy. We demonstrate that overexpression of JMJD6 effectively inhibits ISO-induced increases in cell size and expression of hypertrophic genes, whereas knockdown of JMJD6 aggravates this process, thus indicating that JMJD6 is a critical regulator of cardiomyocyte remodeling. We confirm that JMJD6 can demethylate histone arginine, and H3R8 may be a new histone substrate of JMJD6 demethylation. Importantly, we found that JMJD6 interacts with NF-κB p65 and demethylates its R149 subunit, and prevents the translocation of p65 into the nucleus, thereby reducing the

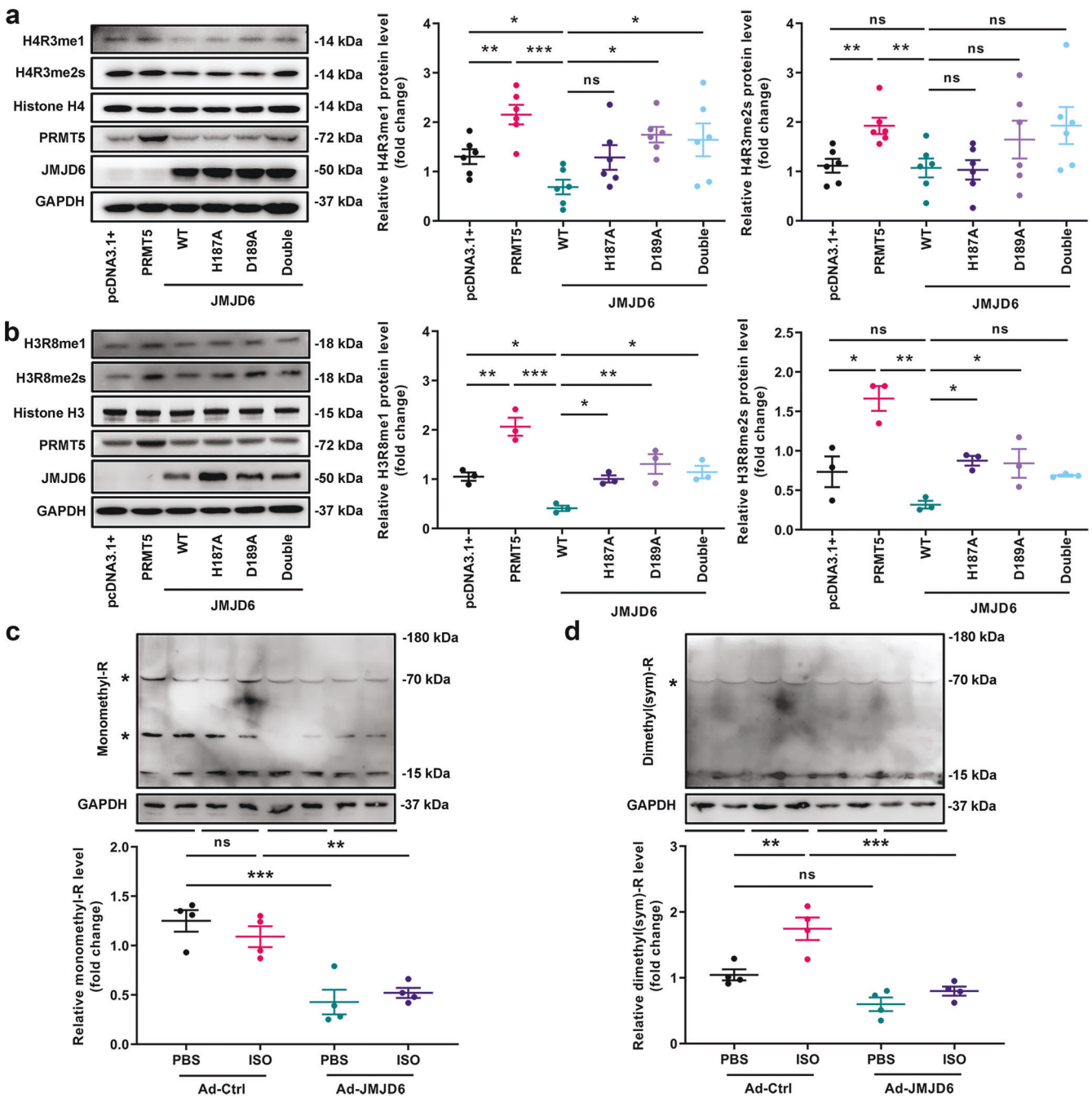

Fig. 6 JMJD6 decreased the methylation level in ISO-induced cardiac hypertrophy. a The histone H4R3 methylation level was detected by Western blot in 293 T cells treated with PRMT5, WT-JMJD6 and mutant-JMJD6 (H187A, D189A or Double) transfection for 48 h. Left: Representative Western blot images showing the expression of H4R3me1 and H4R3me2s. Middle: The quantification of H4R3me1 level. Right: The quantification of H4R3me2s level ($n = 6$). **b** The histone H3R8 methylation level was detected by Western blot in 293 T cells treated with PRMT5, WT-JMJD6 and mutant-JMJD6 (H187A, D189A or Double) transfection for 48 h. Left: Representative Western blot images showing the expression of H3R8me1 and H3R8me2s. Middle: The quantification of H3R8me1 level. Right: The quantification of H3R8me2s level ($n = 3$). **c** Representative Western blot images and quantitative result showing the monomethylation level of arginine (R) in NRCMs infected with Ad-JMJD6 or Ad-Ctrl for 48 h in presence of ISO or PBS ($n = 4$). **d** Representative Western blot images and quantitative result showing the symmertrical dimethylation level of R in NRCMs infected with Ad-JMJD6 or Ad-Ctrl for 48 h in presence of ISO or PBS ($n = 4$). One-way ANOVA with Tukey's correction for multiple comparisons was used in (**a**–**d**). $^{*}P < 0.05$, $^{**}P < 0.01$, $^{***}P < 0.001$, ns not significant.

activation of the NF-κB signaling pathway in the presence of ISO.

It is well known that histone modifications play an important role in gene transcription and heart-related diseases [10]. At present, multiple studies have been conducted regarding histone acetylation and its role in cardiac remodeling [56, 57]. By comparison, the function of histone methylation is relatively poorly understood, even though it is the most common form of histone modifications. Unlike histone acetylation, which mainly occurs on lysine residues, histone methylation not only occurs on lysine but also on arginine residues, making it more complicated than acetylation. Histone methylation can lead to either activation

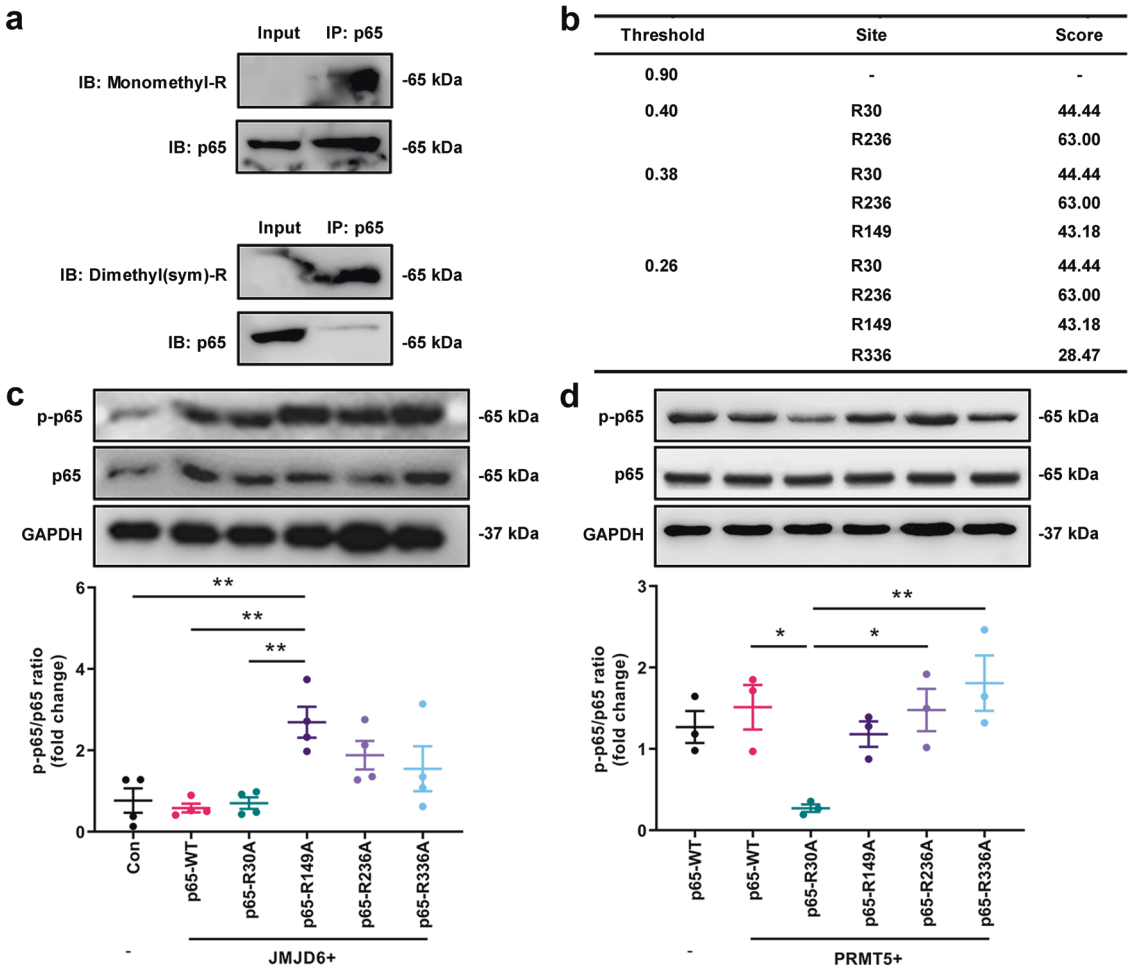

Fig. 7 JMJD6 demethylated R149 of p65 to inactivate NF-κB. a Immunoprecipitation analysis showed the monomethylation and symmertrical dimethylation level of arginine in p65 in NRCMs using p65 antibody. **b** The potential arginine methylation sites in amino acid sequence of *Rattus norvegicus* JMJD6 using a methylation site prediction platform. **c** Representative Western blot images and quantitative result showing p65 phosphorylation at Ser536 in 293 T cells co-transfected with WT-JMJD6 and p65 (WT, R30A, R149A, R236A or R336A) ($n = 4$). **d** Representative Western blot images and quantitative result showing p65 phosphorylation at Ser536 in 293 T cells co-transfected with WT-PRMT5 and p65 (WT, R30A, R149A, R236A or R336A) ($n = 3$). One-way ANOVA with Tukey's correction for multiple comparisons was used in (**c**) and (**d**). $^{*}P < 0.05$, $^{**}P < 0.01$.

or repression of gene transcription, depending on the type of residues, the degree of methylation status (mono-, di-, or trimethylation), and chromatin location [11, 12]. A genome-wide analysis of histone methylation profile in cardiomyocytes of heart failure in both animal models and patients showed that the enzymes responsible for methylation and demethylation of histone H3 lysine 4 (H3K4) and H3K9 may play an important role in cardiac hypertrophy and heart failure [58]. In recent decades, multiple histone methyltransferases (HMTs) and demethylases (HDMs) have been identified. Among them, the JMJD family is an important demethylase family, where JMJD1A [59], JMJD1C [60], and JMJD2A [18, 61] have been confirmed to be involved in cardiac hypertrophy/remodeling. Consistent with previous reports, we observed that the mRNA level of JMJD1A and JMJD2A were reduced in our ISO-induced hypertrophic model (Supplementary Fig. S1e), indicating that alterations of the JMJD family may be similar under various hypertrophic models. Our previous study found that H3K27 mediated by JMJD3 and H4R3 mediated by PRMT5 play an important role in the process of cardiac hypertrophy [15, 19]. In the current study, we discovered that JMJD6 is also involved in cardiac hypertrophy and heart failure.

At present, the use of left ventricular ejection fraction (LVEF) to stratify patients with heart failure is still the most important and accurate clinical method [62]. According to the 2013 ACCF/AHA guideline for the management of heart failure, patients are divided into HFrEF and HFpEF [63]. Interestingly, we found that JMJD6 level was significantly increased in our ISO-induced cardiac hypertrophy and HFpEF model as well as in TAC induced pressure overload model, while it was reduced in patients with HFrEF. Our studies further demonstrated that JMJD6 plays a protective role in ISO-induced hypertrophic model in NRCMs. Furthermore, in parallel with our in vitro results, we observed that cardiac-specific JMJD6 overexpression by intramyocardial injection also significantly attenuates the hypertrophic response induced by ISO and rescues the heart function in SD rats. Although this conclusion seems to be contradictory to the increased expression of JMJD6 seen in hypertrophy (Fig. 1c–g), prolonged hypertrophy will deteriorate cardiac function and eventually lead to heart failure [4], while accompanying with JMJD6 reduction (Fig. 1a, b). According to our findings, the level of JMJD6 is higher in the hypertrophic heart during a compensatory protection period, whereas the expression of JMJD6 is reduced in patients with HFrEF, which could indicate that the levels of JMJD6 are constantly changing in hypertrophic compensation and heart failure. Therefore, we speculate that JMJD6 might be related to the severity of heart-related diseases (Supplementary Fig. S8), and that the

increase of JMJD6 in cardiac hypertrophy is compensatory, and higher level of JMJD6 may be a protective factor in these conditions.

Several lines of evidence supported a strong link between NF-κB signaling and cardiac hypertrophy [52, 53, 64–66]. Our current findings revealed a functional interaction between JMJD6 and NF-κB p65 in cardiomyocytes. JMJD6 was beneficial to weaken the nuclear translocation of p65 under pathological conditions, rather than affecting IκBα degradation. In addition to histone substrate, JMJD6 has been reported to have demethylation modification effects on non-histone proteins (such as ERα, G3BP1 and TRAF6) [24–26], therefore, it is possible that JMJD6 may regulate p65 via demethylation of these non-histone proteins as well. PRMT5 can methylate NF-κB p65 at R30, and its activity can be increased with PRMT5 overexpression [36]. Consistent with this report, our results indicate that p65 was methylated under normal conditions. Furthermore, we predicted more potential arginine methylation modification sites (R149, R236 and R336) of p65 using the prediction platform [49]. The amino acid sequence of these sites is similar to R30, where arginine is always accompanied by a glycine (R-G). It is possible that this structure is required for arginine methylation. In our present studies, we used R30 and PRMT5 as a positive control to test the function of these newly found sites. An important site of phosphorylation of p65 subunit is at Ser536 (p-p65), and this phosphorylation is involved in the regulation of transcriptional activity, nuclear localization and protein stability [54, 67]. Our data shows that p-p65 was markedly increased only by co-transfection of WT-JMJD6 and R149A-p65, indicating that the activity of p65 was amplified due to the mutant in arginine 149 of p65. Considering our previous results, we believe that demethylation of p65 at R149 by JMJD6 could prevent the translocation of p65 into the nucleus, thereby effectively alleviating cardiac hypertrophy. At the same time, we observed that PRMT5 can methylate p65 at R30 to increase its vitality, which is an excellent control for our experiment. These results suggest that the modification of p65 by JMJD6 and PRMT5 occurs at different sites, and they both have an important impact on the activity of p65.

Although we cannot exclude the involvement of other regulating mechanisms in our observations, these results indicate that JMJD6 is indeed a protective factor for pathological cardiac hypertrophy. It will be worth determining in the future whether small molecule agonists designed to target the demethylase activity of JMJD6 are beneficial in improving cardiac function in pathological conditions. Another limitation was that we were not able to detect JMJD6 expression in hypertrophic cardiomyopathy (HCM) samples which were more closely related to our murine model but more difficult to obtain, and instead examined JMJD6 expression in dilated cardiomyopathy (DCM) patients.

CONCLUSIONS

We identify JMJD6 as a cardioprotective demethylase. JMJD6 prevents ISO-induced pathological cardiac hypertrophy by demethylating p65 subunit at site R149 to reduce NF-κB signaling. These findings improve our understanding of pathological cardiac hypertrophy and epigenetic modification. Considering this, targeting JMJD6 is a potential target for therapeutic interventions for pathological cardiac hypertrophy.

ACKNOWLEDGEMENTS

ZG was supported by the American Heart Association Postdoctoral Fellowship (898679). JL was supported by National Natural Science Foundation of China (82173808), Natural Science Foundation of Guangdong Province (2021B1515020100) and Guangzhou Basic and Applied Basic Research Project (202102020173). WWL was supported by National Natural Science Foundation of China (82003746). PQL was supported by National Natural Science Foundation of China (U21A20419, 81872860), Local Innovative and Research Teams Project of Guangdong Pearl River Talents Program (2017BT01Y093), and National Engineering and Technology Research Center for New drug Druggability Evaluation (Seed Program of Guangdong Province, 2017B090903004). JGZ was supported by Academic Promotion Program of Shandong First Medical University (2019LJ003). LW was supported by the Project of Shandong Medical and Health Science and Technology (202002040923).

AUTHOR CONTRIBUTIONS

ZG and YHH performed the study, analyzed the data, wrote and revised the manuscript. GSF, ZZL, SDC, QQW and WWL contributed to the animal experiments. GSF, QL, LYL, LW and JGZ contributed to the acquisition of data and data interpretation. CVR contributed to the language polish. AJ provided the TAC mice cardiac tissues. ZKW provided heart tissues from humans with heart failure. ZG, JL and PQL made the hypothesis and participated in the experimental design, and manuscript preparation. All authors approved the final version of the manuscript.

ADDITIONAL INFORMATION

Supplementary information The online version contains supplementary material available at https://doi.org/10.1038/s41401-023-01086-7.

Competing interests: The authors declare no competing interests.

REFERENCES

1. Virani SS, Alonso A, Benjamin EJ, Bittencourt MS, Callaway CW, Carson AP, et al. Heart disease and stroke statistics-2020 update: a report from the American Heart Association. Circulation. 2020;141:e139–e596.
2. Frey N, Katus HA, Olson EN, Hill JA. Hypertrophy of the heart: a new therapeutic target? Circulation. 2004;109:1580–9.
3. Maillet M, van Berlo JH, Molkentin JD. Molecular basis of physiological heart growth: fundamental concepts and new players. Nat Rev Mol Cell Biol. 2013;14:38–48.
4. MacDonald MR, Petrie MC, Hawkins NM, Petrie JR, Fisher M, McKelvie R, et al. Diabetes, left ventricular systolic dysfunction, and chronic heart failure. Eur Heart J. 2008;29:1224–40.
5. Mano H. Epigenetic abnormalities in cardiac hypertrophy and heart failure. Environ Health Prev Med. 2008;13:25–29.
6. Lin Z, Li Z, Guo Z, Cao Y, Li J, Liu P, et al. Epigenetic reader bromodomain containing protein 2 facilitates pathological cardiac hypertrophy via regulating the expression of citrate cycle genes. Front Pharmacol. 2022;13:887991.
7. Liu CF, Tang WHW. Epigenetics in cardiac hypertrophy and heart failure. JACC Basic Transl Sci. 2019;4:976–93.
8. Li Q, Li ZM, Sun SY, Wang LP, Wang PX, Guo Z, et al. PARP1 interacts with HMGB1 and promotes its nuclear export in pathological myocardial hypertrophy. Acta Pharmacol Sin. 2019;40:589–98.
9. Li Z, Guo Z, Lan R, Cai S, Lin Z, Li J, et al. The poly(ADP-ribosyl)ation of BRD4 mediated by PARP1 promoted pathological cardiac hypertrophy. Acta Pharm Sin B. 2021;11:1286–99.
10. Greer EL, Shi Y. Histone methylation: a dynamic mark in health, disease and inheritance. Nat Rev Genet. 2012;13:343–57.
11. Bannister AJ, Kouzarides T. Reversing histone methylation. Nature. 2005;436:1103–6.
12. Bannister AJ, Kouzarides T. Regulation of chromatin by histone modifications. Cell Res. 2011;21:381–95.
13. Zhao Z, Shilatifard A. Epigenetic modifications of histones in cancer. Genome Biol. 2019;20:245.
14. Peter CJ, Akbarian S. Balancing histone methylation activities in psychiatric disorders. Trends Mol Med. 2011;17:372–9.
15. Cai S, Wang P, Xie T, Li Z, Li J, Lan R, et al. Histone H4R3 symmetric di-methylation by prmt5 protects against cardiac hypertrophy via regulation of Filip1L/beta-catenin. Pharmacol Res. 2020;161:105104.
16. Pyun JH, Kim HJ, Jeong MH, Ahn BY, Vuong TA, Lee DI, et al. Cardiac specific PRMT1 ablation causes heart failure through CaMKII dysregulation. Nat Commun. 2018;9:5107.
17. Zhang QJ, Liu ZP. Histone methylations in heart development, congenital and adult heart diseases. Epigenomics. 2015;7:321–30.
18. Zhang QJ, Chen HZ, Wang L, Liu DP, Hill JA, Liu ZP. The histone trimethyllysine demethylase JMJD2A promotes cardiac hypertrophy in response to hypertrophic stimuli in mice. J Clin Invest. 2011;121:2447–56.
19. Guo Z, Lu J, Li J, Wang P, Li Z, Zhong Y, et al. JMJD3 inhibition protects against isoproterenol-induced cardiac hypertrophy by suppressing beta-MHC expression. Mol Cell Endocrinol. 2018;477:1–14.

20. Chang B, Chen Y, Zhao Y, Bruick RK. JMJD6 is a histone arginine demethylase. Science. 2007;318:444–7.
21. Liu W, Ma Q, Wong K, Li W, Ohgi K, Zhang J, et al. Brd4 and JMJD6-associated anti-pause enhancers in regulation of transcriptional pause release. Cell. 2013;155:1581–95.
22. Unoki M, Masuda A, Dohmae N, Arita K, Yoshimatsu M, Iwai Y, et al. Lysyl 5-hydroxylation, a novel histone modification, by Jumonji domain containing 6 (JMJD6). J Biol Chem. 2013;288:6053–62.
23. Webby CJ, Wolf A, Gromak N, Dreger M, Kramer H, Kessler B, et al. Jmjd6 catalyses lysyl-hydroxylation of U2AF65, a protein associated with RNA splicing. Science. 2009;325:90–93.
24. Poulard C, Rambaud J, Hussein N, Corbo L, Le Romancer M. JMJD6 regulates ERalpha methylation on arginine. PLoS One. 2014;9:e87982.
25. Tikhanovich I, Kuravi S, Artigues A, Villar MT, Dorko K, Nawabi A, et al. Dynamic arginine methylation of tumor necrosis factor (TNF) receptor-associated factor 6 regulates toll-like receptor signaling. J Biol Chem. 2015;290:22236–49.
26. Tsai WC, Reineke LC, Jain A, Jung SY, Lloyd RE. Histone arginine demethylase JMJD6 is linked to stress granule assembly through demethylation of the stress granule-nucleating protein G3BP1. J Biol Chem. 2017;292:18886–96.
27. Vrankova S, Barta A, Klimentova J, Dovinova I, Liskova S, Dobesova Z, et al. The regulatory role of nuclear factor kappa B in the heart of hereditary hypertriglyceridemic rat. Oxid Med Cell Longev. 2016;2016:9814038.
28. Huxford T, Huang DB, Malek S, Ghosh G. The crystal structure of the IkappaBalpha/NF-kappaB complex reveals mechanisms of NF-kappaB inactivation. Cell. 1998;95:759–70.
29. Jacobs MD, Harrison SC. Structure of an IkappaBalpha/NF-kappaB complex. Cell. 1998;95:749–58.
30. Huang B, Yang XD, Lamb A, Chen LF. Posttranslational modifications of NF-kappaB: another layer of regulation for NF-kappaB signaling pathway. Cell Signal. 2010;22:1282–90.
31. Lu T, Stark GR. NF-kappaB: regulation by methylation. Cancer Res. 2015;75:3692–5.
32. Ea CK, Baltimore D. Regulation of NF-kappaB activity through lysine monomethylation of p65. Proc Natl Acad Sci USA. 2009;106:18972–7.
33. Levy D, Kuo AJ, Chang Y, Schaefer U, Kitson C, Cheung P, et al. Lysine methylation of the NF-kappaB subunit RelA by SETD6 couples activity of the histone methyltransferase GLP at chromatin to tonic repression of NF-kappaB signaling. Nat Immunol. 2011;12:29–36.
34. Lu T, Jackson MW, Wang B, Yang M, Chance MR, Miyagi M, et al. Regulation of NF-kappaB by NSD1/FBXL11-dependent reversible lysine methylation of p65. Proc Natl Acad Sci USA. 2010;107:46–51.
35. Yang XD, Huang B, Li M, Lamb A, Kelleher NL, Chen LF. Negative regulation of NF-kappaB action by Set9-mediated lysine methylation of the RelA subunit. EMBO J. 2009;28:1055–66.
36. Wei H, Wang B, Miyagi M, She Y, Gopalan B, Huang DB, et al. PRMT5 dimethylates R30 of the p65 subunit to activate NF-kappaB. Proc Natl Acad Sci USA. 2013;110:13516–21.
37. Hu Y, Guo Z, Lu J, Wang P, Sun S, Zhang Y, et al. sFRP1 has a biphasic effect on doxorubicin-induced cardiotoxicity in a cellular location-dependent manner in NRCMs and Rats. Arch Toxicol. 2019;93:533–46.
38. Liang L, Tu Y, Lu J, Wang P, Guo Z, Wang Q, et al. Dkk1 exacerbates doxorubicin-induced cardiotoxicity by inhibiting the Wnt/beta-catenin signaling pathway. J Cell Sci. 2019;132:jcs228478.
39. Sun S, Hu Y, Zheng Q, Guo Z, Sun D, Chen S, et al. Poly(ADP-ribose) polymerase 1 induces cardiac fibrosis by mediating mammalian target of rapamycin activity. J Cell Biochem. 2019;120:4813–26.
40. Wang P, Lan R, Guo Z, Cai S, Wang J, Wang Q, et al. Histone demethylase JMJD3 mediated doxorubicin-induced cardiomyopathy by suppressing SESN2 expression. Front Cell Dev Biol. 2020;8:548605.
41. Li J, Huang J, Lu J, Guo Z, Li Z, Gao H, et al. Sirtuin 1 represses PKC-zeta activity through regulating interplay of acetylation and phosphorylation in cardiac hypertrophy. Br J Pharmacol. 2019;176:416–35.
42. Lu J, Li J, Hu Y, Guo Z, Sun D, Wang P, et al. Chrysophanol protects against doxorubicin-induced cardiotoxicity by suppressing cellular PARylation. Acta Pharm Sin B 2019;9:782–93.
43. Guo Z, Liao Z, Huang L, Liu D, Yin D, He M. Kaempferol protects cardiomyocytes against anoxia/reoxygenation injury via mitochondrial pathway mediated by SIRT1. Eur J Pharmacol. 2015;761:245–53.
44. Li Z, Zhang X, Guo Z, Zhong Y, Wang P, Li J, et al. SIRT6 suppresses NFATc4 expression and activation in cardiomyocyte hypertrophy. Front Pharmacol. 2018;9:1519.
45. Guo Z, Valenzuela Ripoll C, Picataggi A, Rawnsley D, Ozcan M, Chirinos J, et al. Apolipoprotein M attenuates anthracycline cardiotoxicity and lysosomal injury. JACC Basic Transl Sci. 2023;8:340–55.
46. Ozcan M, Guo Z, Valenzuela Ripoll C, Diab A, Picataggi A, Rawnsley D, et al. Sustained alternate day fasting potentiates doxorubicin cardiotoxicity. Cell Metab. 2023. Online ahead of print. https://doi.org/10.1016/j.cmet.2023.02.006.
47. Guo Z, Zhang Y, Liu C, Youn JY, Cai H. Toll-like receptor 2 (TLR2) knockout abrogates diabetic and obese phenotypes while restoring endothelial function via inhibition of NOX1. Diabetes. 2021;70:2107–19.
48. Luo W, Wang Y, Yang H, Dai C, Hong H, Li J, et al. Heme oxygenase-1 ameliorates oxidative stress-induced endothelial senescence via regulating endothelial nitric oxide synthase activation and coupling. Aging (Albany NY). 2018;10:1722–44.
49. Chen H, Xue Y, Huang N, Yao X, Sun Z. MeMo: a web tool for prediction of protein methylation modifications. Nucleic Acids Res. 2006;34:W249–W253.
50. Javan H, Szucsik AM, Li L, Schaaf CL, Salama ME, Selzman CH. Cardiomyocyte p65 nuclear factor-kappaB is necessary for compensatory adaptation to pressure overload. Circ Heart Fail. 2015;8:109–18.
51. Gupta S, Young D, Maitra RK, Gupta A, Popovic ZB, Yong SL, et al. Prevention of cardiac hypertrophy and heart failure by silencing of NF-kappaB. J Mol Biol. 2008;375:637–49.
52. Hong HQ, Lu J, Fang XL, Zhang YH, Cai Y, Yuan J, et al. G3BP2 is involved in isoproterenol-induced cardiac hypertrophy through activating the NF-kappaB signaling pathway. Acta Pharmacol Sin. 2018;39:184–94.
53. Yu SS, Cai Y, Ye JT, Pi RB, Chen SR, Liu PQ, et al. Sirtuin 6 protects cardiomyocytes from hypertrophy in vitro via inhibition of NF-kappaB-dependent transcriptional activity. Br J Pharmacol. 2013;168:117–28.
54. Sakurai H, Chiba H, Miyoshi H, Sugita T, Toriumi W. IkappaB kinases phosphorylate NF-kappaB p65 subunit on serine 536 in the transactivation domain. J Biol Chem. 1999;274:30353–6.
55. Sasaki CY, Barberi TJ, Ghosh P, Longo DL. Phosphorylation of RelA/p65 on serine 536 defines an I{kappa}B{alpha}-independent NF-{kappa}B pathway. J Biol Chem. 2005;280:34538–47.
56. Backs J, Olson EN. Control of cardiac growth by histone acetylation/deacetylation. Circ Res. 2006;98:15–24.
57. Ooi JY, Tuano NK, Rafehi H, Gao XM, Ziemann M, Du XJ, et al. HDAC inhibition attenuates cardiac hypertrophy by acetylation and deacetylation of target genes. Epigenetics. 2015;10:418–30.
58. Papait R, Cattaneo P, Kunderfranco P, Greco C, Carullo P, Guffanti A, et al. Genome-wide analysis of histone marks identifying an epigenetic signature of promoters and enhancers underlying cardiac hypertrophy. Proc Natl Acad Sci USA. 2013;110:20164–9.
59. Zang R, Tan Q, Zeng F, Wang D, Yu S, Wang Q. JMJD1A represses the development of cardiomyocyte hypertrophy by regulating the expression of catalase. Biomed Res Int. 2020;2020:5081323.
60. Yu S, Li Y, Zhao H, Wang Q, Chen P. The Histone demethylase JMJD1C regulates CAMKK2-AMPK signaling to participate in cardiac hypertrophy. Front Physiol. 2020;11:539.
61. Rosales W, Lizcano F. The histone demethylase JMJD2A modulates the induction of hypertrophy markers in iPSC-derived cardiomyocytes. Front Genet. 2018;9:14.
62. Bristow MR, Kao DP, Breathett KK, Altman NL, Gorcsan J 3rd, Gill EA, et al. Structural and functional phenotyping of the failing heart: Is the left ventricular ejection fraction obsolete? JACC Heart Fail. 2017;5:772–81.
63. Yancy CW, Jessup M, Bozkurt B, Butler J, Casey DE Jr, Drazner MH, et al. 2013 ACCF/AHA guideline for the management of heart failure: executive summary: a report of the American College of Cardiology Foundation/American Heart Association Task Force on practice guidelines. Circulation. 2013;128:1810–52.
64. Purcell NH, Tang G, Yu C, Mercurio F, DiDonato JA, Lin A. Activation of NF-kappa B is required for hypertrophic growth of primary rat neonatal ventricular cardiomyocytes. Proc Natl Acad Sci USA. 2001;98:6668–73.
65. Zelarayan L, Renger A, Noack C, Zafiriou MP, Gehrke C, van der Nagel R, et al. NF-kappaB activation is required for adaptive cardiac hypertrophy. Cardiovasc Res. 2009;84:416–24.
66. Zou J, Li H, Chen X, Zeng S, Ye J, Zhou C, et al. C/EBPbeta knockdown protects cardiomyocytes from hypertrophy via inhibition of p65-NFkappaB. Mol Cell Endocrinol. 2014;390:18–25.
67. Sizemore N, Lerner N, Dombrowski N, Sakurai H, Stark GR. Distinct roles of the Ikappa B kinase alpha and beta subunits in liberating nuclear factor kappa B (NF-kappa B) from Ikappa B and in phosphorylating the p65 subunit of NF-kappa B. J Biol Chem. 2002;277:3863–9.